Accepted Manuscript

Title: Quick and efficient co-treatment of Zn^{2+}/Ni^{2+} and CN^- via the formation of $Ni(CN)_4^{2-}$ intercalated larger ZnAl-LDH crystals

Author: Ji Zhi Zhou Ying Liang Jia Zhang Li Li Yunfeng Xu Xiuxiu Ruan Guangren Qian Zhi Ping Xu

Please cite this article as: J.Z. Zhou, Y. Liang, J. Zhang, L. Li, Y. Xu, X. Ruan, G. Qian, Z.P. Xu, Quick and efficient co-treatment of Zn^{2+}/Ni^{2+} and CN^{minus} via the formation of $Ni(CN)_4^{2minus}$</sup> intercalated larger ZnAl-LDH crystals, *Journal of Hazardous Materials* (2014), http://dx.doi.org/10.1016/j.jhazmat.2014.07.001

Quick and efficient co-treatment of Zn^{2+}/Ni^{2+} and CN^- via the formation of $Ni(CN)_4^{2-}$ intercalated larger ZnAl-LDH crystals

Ji Zhi Zhou[a], Ying Liang[a], Jia Zhang[a], Li Li[b], Yunfeng Xu[a], Xiuxiu Ruan[a], Guangren Qian[a,*], and Zhi Ping Xu[a,b,**]

[a] School of Environmental and Chemical Engineering, Shanghai University, No.99 Shangda Rd., Shanghai 200444, P. R. China;

[b] ARC Centre of Excellence for Functional Nanomaterials, Australian Institute of Bioengineering and Nanotechnology, The University of Queensland, Brisbane, QLD 4072, Australia

[*] Phone: 86 21 66137758; Fax: 86 21 56333052; e-mail: grqian@shu.edu.cn.

[**] Phone: +61 7 33463809; Fax :+61 7 33463973. e-mail: gordonxu@uq.edu.au;

1

Highlights

A quick treatment was developed to simultaneously purify aqueous CN and heavy metals

Conversion of $Zn(CN)_4^{2-}$ to $Ni(CN)_4^{2-}$ occurred when Ni^{2+} was added in Zn/CN solutions

Over 95% of CN was removed as $Ni(CN)_4^{2-}$ intercalated ZnAl-LDH formation with Al added

CN removal can also be improved by CN encapsulation in ZnAl-LDH that has large size

ABSTRACT: The wide use of metal electroplating involving CN^- necessitates the cost-effective treatment of both CN and metals (Zn, Cu, Ni etc.). In this research, we developed a novel strategy - Ni^{2+}-assisted layered double hydroxide (LDH) precipitation - to simultaneously remove aqueous CN and Zn/Ni metals. The strategy is to convert $CN^-/Zn(CN)_4^{2-}$ to $Ni(CN)_4^{2-}$ first, and then to quickly precipitate $Ni(CN)_4^{2-}/CN^-$ into LDH crystals. The conversion has been clearly evidenced by the change of CN characteristic FTIR bands of Zn-CN solution before and after adding $Ni(NO_3)_2$. The intercalation and efficient removal of CN have also been confirmed through the formation of LDH crystals XRD and SEM. In particular, a set of optimized experimental factors has been obtained by investigating their effects on CN

2

removal efficiency in the simulated tests. Remarkably, over 95% CN were removed with high removal efficiencies of metals. Our results thus suggest that the current strategy is a quick, efficient and promising way to simultaneously treat both Ni and metals/CN rich electroplating wastewaters.

3

1. Introduction

Layered double hydroxide (LDH) is a family of anionic clay, which is commonly represented by the formula $M^{2+}_{(1-x)}M^{3+}_x(OH)_2A^{n-}_{(x/n)}\cdot mH_2O$, attracts wide investigations in applications to environment, biomedicine, and catalysis [1-4]. LDH allows the synchronous incorporation of multiple bivalent and trivalent cations (M^{2+} and M^{3+}) into the brucite-like layer with different molar ratios ($x = 0.2$-0.4) [5, 6]. Thus, various heavy metals can be removed efficiently from electroplating wastewaters by precipitation of polynary metals contained LDH [7, 8]. Apart from cations, anions (A^{n-}) are also intercalated into LDH interlayer synchronously when LDH is formed. For instance, when Zn(II)-Ni(II)-Cr(III)-LDH was precipitated in a CN-bearing wastewater by mixing with Fe contained pickle acid liquors, co-existing CN^- and $Fe(CN)_6^{4-}$ were removed by adsorption or intercalation into LDH [9]. This result suggests that co-precipitation of LDH is a promising way to remove metals and anions simultaneously from wastewaters.

Although cyanide (CN^-) is very toxic to animals and humans [10], it is still often used in the electroplating industries (e.g. Zn-CN and Cu-CN electroplating) to assure the high quality of electroplating. To meet the strict regulations for discharge of these wastewaters, cost-effective treatment for such wastewaters is urgently necessary. There are several technologies to treat CN-bearing wastewaters, including commonly used alkaline chlorination, chemical complex precipitation, adsorption, and ion-exchange [11-13]. However, numerous disadvantages, such as high cost, toxic byproduct (CNCl), low efficiency and recycle difficulty of adsorbent, limit these

4

methods in the treatment of CN-bearing wastewaters. Previously, we used co-precipitation of polynary metals-LDHs to treat CN-bearing wastewaters, and only ~50% CN^- was removed. We then used pickle acid liquors (contained Fe^{2+}) to mix with the CN-bearing wastewater in order to convert CN^- to $Fe(CN)_6^{4-}$ first and remove CN via forming $Fe(CN)_6^{4-}$-LDH, since $Fe(CN)_6^{4-}$ had a stronger affinity for LDH interlayer than free CN^- [14]. Unfortunately, the conversion of free CN^- to $Fe(CN)_6^{4-}$ was very limited and the CN removal efficiency was not significantly enhanced [9].

On the other hand, an alternative transition of free CN^- to complex could be achieved by adding Ni^{2+}, which would increase the removal of CN^-. This hypothesis is based on the following reasons: (1) $Ni(CN)_4^{2-}$ has a relatively high cumulative formation constant ($log\beta4$) which is almost the same with that of $Fe(CN)_6^{4-}$ (31.3 for $Ni(CN)_4^{2-}$ vs. 35.0 for $Fe(CN)_6^{4-}$) [15]; (2) transition from CN^- to $Ni(CN)_4^{2-}$ is easier, since it involves less CN^- (4 vs. 6 in $Fe(CN)_6^{4-}$); (3) square planar $Ni(CN)_4^{2-}$ is easier to be intercalated into LDH interlayer at a high charge density (such as $M^{2+}/M^{3+}= 2:1$) in LDH as there is no need to expand the interlayer spacing during the formation of LDH[16]. Moreover, the industrial CN-bearing wastewater often contains abundant heavy metals, such as Zn and Cu [17, 18]. Since the addition of Ni is a promising way to convert free CN^- into $Ni(CN)_4^{2-}$ and remove CN^- from wastewater, an Ni rich wastewater is suggested as the alternative Ni source in this novel CN removal strategy to treat two or more wastewaters simultaneously [9].

Therefore, a feasible approach to co-treatment of aqueous CN/metals is proposed using Ni^{2+}-assisted LDH precipitation. The objectives of this work were to (1)

5

evaluate the removal efficiency of CN and metals from CN/metals bearing solution with or without Ni^{2+} addition pre-treated; (2) identify the formation of $Ni(CN)_4^{2-}$ and its intercalation into LDH; and (3) optimize the conditions to maximize CN removal. Excitedly, 95% CN was removed in the treatment of CN^-/metals solution containing 5-25 mg/L of CN.

2. Materials and methods

2.1. Materials. Chemicals such as NaOH, $Ni(NO_3)_2 \cdot 6H_2O$, $Zn(CN)_2$, KCN, $Zn(NO_3)_2 \cdot 6H_2O$ and $Al(NO_3)_3 \cdot 9H_2O$ were purchased from Sinopharm Group Chemical Reagent Co. Ltd., China, and directly used without further purification.

2.2. Removal of CN from Zn-CN Solution. The demonstration of CN removal by Ni^{2+}-assisted LDH co-precipitation was performed in a simulated solution with 25.0 mg/L (0.96 mmol/L) of total CN and 15.6 mg/L of Zn (0.24 mmol/L), which was prepared by dissolving KCN and $Zn(CN)_2$ at pH 12.0. Typically, 10 ml solution containing 14.1 mg $Ni(NO_3)_2 \cdot 6H_2O$ (Ni^{2+} = 0.048 mmol) was added in 200 mL of simulated solution at pH 12.0 prior to LDH co-precipitation. Ni/CN molar ratio was 1:4. After mixing with 10 mL of a metal solution (Zn^{2+} = 0.769 mmol, Al^{3+} = 0.384 mmol), the pH value of mixed solution was adjusted at around 8.0 by adding diluted $NaOH/HNO_3$ solution after precipitation. Non-toxic Al^{3+} was introduced for LDH precipitation, where extra Zn^{2+} was added to keep the total Zn/Al=2.0 in the initial solution. Since the precipitation is a quick process, LDH is formed in a short time

6

(usually 10 min). On the other hand, the intercalation of anion into LDH took much time (several hours). Accordingly, the kinetics experiment was carried out for 10 min to 18 hr for the performance of Ni-CN complex removal by LDH precipitation.

The precipitate was collected via centrifugation, and dried at 80 ^{o}C in a vacuum oven for further characterization. The solid sample after treatment was then denoted as Zn_2Al-LDH. The supernatant was stored in a high density polyethylene (HDPE) bottle for the determination of pH and the concentrations of residual metals and CN.

Moreover, effects of stirring time, pH and CN/Al molar ratio were examined in the similar way, in order to optimize the Ni-assisted treatment conditions for simultaneous removal of CN and metals from the Zn-CN solution. Scheme 1 shows the block diagram of the treatment steps, sequence and the associated conditions.

2.3. Preparation of Zn_2Al-CO_3-LDH and Zn_2Al-$Ni(CN)_4$-LDH. Zn_2Al-CO_3-LDH and Zn_2Al-$Ni(CN)_4$-LDH were prepared by the co-precipitation method. Briefly, 100 ml mixed solution containing 10 mmol $Zn(NO_3)_2 \cdot 6H_2O$ and 5 mmol $Al(NO_3)_3 \cdot 9H_2O$ was added to a solution containing 30 mmol NaOH or 30 mmol NaOH together with 2.5 mmol $K_2Ni(CN)_4 \cdot 1.8H_2O$. The resultant suspension was stirred for 18 h (the latter was under N_2 atmosphere). The precipitate was collected via centrifugation, thoroughly washed with deionized water and dried at 80 ^{o}C in a vacuum oven for further characterization.

2.4. Characterization. XRD patterns of LDHs were collected on a Rigaku D/max

7

RBX X-ray diffractometer with Cu-K radiation (λ= 0.15406 nm) at a scanning rate of 4°/min in the 2θ range of 5-80°. Fourier Transform Infrared (FTIR) spectra in the range of 400 to 4000 cm^{-1} were recorded on a Nicolet 380 spectrometer (Thermo Scientific Co.) after 128 scans at a resolution of 4 cm^{-1} by measuring the IR absorbance of KBr disc containing 1-2 wt% of sample. The FTIR spectrum of liquid was performed on a liquid film of sample that was held by clipping two pieces of CaF_2 discs.

Metal contents in various solutions and precipitates (by dissolving in acid solution) were determined by inductively coupled plasma atoms emission spectrometer (ICP-AES, Leeman Co., USA). Total CN concentration in wastewater and supernatant was determined by spectrophotometer method [19] after cyanide distillation in a UNICO UV-spectrophotometer (4802UV/VIS), while free CN^- concentration was determined by spectrophotometer without cyanide distillation.

3. Results and discussion

3.1. Removal of CN/metals with or without Ni addition

As listed in Table 1, direct precipitation of Zn_2Al-LDH in Zn-CN solution, e.g. without Ni addition, left 7.41 mg/L of CNt (total CN) in the residual solution with 49% in the form of CNf (free CN^-). In sharp contrast, adding Ni^{2+} and following by precipitation of Zn_2Al-LDH resulted in only 1.19 mg/L of CNt being left in solution. This means that CNt removal efficiency was increased from 70% to 95%. Removal of CNt generally depends on the treatment condition. When the aging time was extended
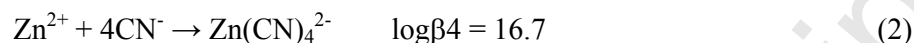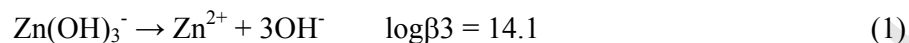
8

from 10 min to 18 h, CNt increased to 5.95 mg/L, indicating that some adsorbed/intercalated $CN^-/Ni(CN)_4^{2-}$ leached out from the LDH to the aqueous phase. The CN leaching could be mainly contributed to the desorption/de-intercalation of CNf from $Zn_2Al-Ni(CN)_4^{2-}$ and CN^--LDH, since the percentage of CNf increased from 15% to 53%, when the total residual CN increased from 1.19 to 5.95 mg/L (Table 1).

Moreover, removal efficiency of metal is also listed in Table 1, showing that over 85% of Zn and Al were removed without Ni^{2+} addition. In comparison, higher removal efficiencies of Zn and Al were observed with Ni^{2+} being added. Especially, over 95% of Zn and Al were precipitated in 18 h, indicating that the long aging time improved the precipitation of Zn_2Al-LDH. However, 72-73% of Ni was removed regardless of the aging time. Compared to that of Zn or Al, the lower Ni removal percentage suggested different removal processes. Interestingly, the molar ratio of removed CN/Ni was 4.1-4.4, close to the theoretical value of 4.0 in $Ni(CN)_4^{2-}$ complex. Accordingly, it was supposed that the formation of $Ni(CN)_4^{2-}$ was responsible for the Ni^{2+} removal and the Zn was mainly removed by forming $ZnAl-Ni(CN)_4$-LDH during LDH precipitation

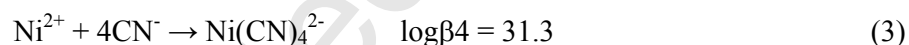## 3.2. Conversion of $Zn(CN)_4^{2-}$ to $Ni(CN)_4^{2-}$.

The first two rows in Table 1 list metal concentrations, CNt concentration and percentage of CNf to CNt before and after Ni addition into Zn-CN solution at pH=12. CNt was 25.0 mg/L, with 55.8% being CNf. This indicated that 44.2% CNt was in the

9

form of CN-complex, such as $Zn(CN)_4^{2-}$, which may transform in the following process:

$$Zn(OH)_3^- \rightarrow Zn^{2+} + 3OH^- \qquad \log\beta3 = 14.1 \qquad (1)$$

$$Zn^{2+} + 4CN^- \rightarrow Zn(CN)_4^{2-} \qquad \log\beta4 = 16.7 \qquad (2)$$

At pH=12, Zn^{2+} ion mainly exists in the form of $Zn(OH)_3^-$. The molar ratio of CNc(CN-complex)/Zn was 1.9, indicating that ~50% Zn^{2+} was bound with CN^- and the other half was probably in the form of $Zn(OH)_3^-$ in the current case.

After adding $Ni(NO_3)_2$ (aq) into Zn-CN solution (Ni/CNt molar ratio was 1:4), CNt was 24.8 mg/L, and the percentage of CNf was decreased to 18.0%. This observation indicated that 37.8% (9.45 mg/L) of CNf was converted to aqueous CNc, very likely via the coordination with Ni^{2+}:

$$Ni^{2+} + 4CN^- \rightarrow Ni(CN)_4^{2-} \qquad \log\beta4 = 31.3 \qquad (3)$$

Moreover, CNc/Ni molar ratio was 3.4, close to the theoretical value of 4.0 in $Ni(CN)_4^{2-}$. This similarity demonstrated that adding Ni^{2+} resulted in not only the coordination of CNf with Ni^{2+} (Eq 3), but also the apparent conversion of $Zn(CN)_4^{2-}$ to $Ni(CN)_4^{2-}$, as the cumulative formation constant ($\beta4$) of $Zn(CN)_4^{2-}$ is less than that of $Ni(CN)_4^{2-}$ by a factor of $10^{14.6}$ [20]:

$$Ni^{2+} + Zn(CN)_4^{2-} \rightarrow Ni(CN)_4^{2-} + Zn^{2+} \qquad (4)$$
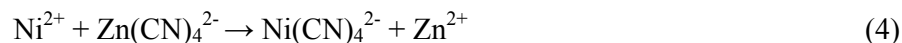
$$K = \beta4(Ni(CN)_4^{2-})/\beta4(Zn(CN)_4^{2-}) = 10^{14.6}$$

The formation of $Ni(CN)_4^{2-}$ via Eqs 3 and 4 has been confirmed by FTIR spectra of CN in aqueous solution before and after Ni^{2+} addition. As shown in Figure 1, KCN

10

solution had a broad peak at 2080 cm^{-1}, and Zn-CN solution had one strong band at 2150 cm^{-1}, attributed to the CN stretching vibration of CNf [20] and $Zn(CN)_4^{2-}$ [21], respectively. After adding Ni^{2+}, the band at 2150 cm^{-1} disappeared together with the appearance of a new strong band at 2123 cm^{-1}, which was assigned to the CN stretching vibration of $Ni(CN)_4^{2-}$ [22]. Furthermore, there was one weak band at 2090 cm^{-1} in the spectrum of Zn-CN solution, which also disappeared after adding Ni^{2+}. This band was owned to the CN stretching vibration of CNf [20]. Thus the change of FTIR spectra clearly indicated the conversion of $Zn(CN)_4^{2-}$ to $Ni(CN)_4^{2-}$ (Eq 4) and the coordination of free CN$^-$ with Ni^{2+} (Eq 3).

It is worth mentioning that there was some $Ni(OH)_2$ precipitation, when more $Ni(NO_3)_2$ was added, which might also occur to a small extent even at the Ni/CNt molar ratio of 1:4, as suggested by the Ni/CNc molar ratio (1:3.4).

3.3. Characterization of CN intercalation with Ni addition

Top two curves in Figure 2 are the XRD patterns of collected samples that were formed after mixing Zn and Al solution with Zn-CN solution, which was pre-treated with $Ni(NO_3)_2$ for 10 min and 18 h. These two patterns revealed the formation of Zn_2Al-LDH intercalated with CO_3^{2-} and $Ni(CN)_4^{2-}$. As also shown by the bottom XRD pattern of ZnAl-LDH, the characteristic diffraction peaks could be observed at 11.6^o, 23.4^o, 34.6^o, 60.0^o and 61.6^o (2θ) that were well indexed, giving lattice parameters a = 0.306 nm and c = 2.268 nm (3d$_{003}$), which was consistent with the reported value for typical Mg_2Al-CO_3-LDH [5]. The major anion was CO_3^{2-} (peak at

11

1355 cm^{-1}) while there would be some intercalated NO$_3^-$ with characteristic peak at 1383 cm^{-1} (Figure 3) [5]. Similarly, the XRD pattern of Zn$_2$Al-Ni(CN)$_4$-LDH (Figure 2) showed that 2θ of characteristic diffraction peaks moved to smaller angles, indicating that the interlayer spacing was expanded, with a = 0.306 nm and c = 3.252 nm (3d$_{003}$).

As shown in Figure 4A, the SEM image of Zn$_2$Al-LDH exhibited a homogeneous morphology of layer-shaped particles, supporting the formation of LDH. Furthermore, spacing arrangement of intercalated Ni(CN)$_4^{2-}$ in the Zn$_2$Al-LDH interlayer could be tilted. As shown in Figure 4B, the height of Ni(CN)$_4^{2-}$ was 0.61 nm as the d-spacing of Zn$_2$Al-Ni(CN)$_4$-LDH was 1.09 nm and the thickness of brucite-like layer was 0.48 nm. Since the side length of Ni(CN)$_4^{2-}$ square is about 0.43 nm, the following relationship is established by considering the van del Waal's radius of N (0.14 nm):

$$0.61 = 0.28 + 0.43 \sin\theta \tag{5}$$

e.g. the tilting angle was 51°, which was similar to the result in the case of MgAl-LDH [16]. Consistently, Ni(CN)$_4^{2-}$ intercalation was also evidenced by the peak at 2121 cm^{-1} in Figure 3. Obviously, the XRD patterns of samples collected from simulated solution contained both Zn$_2$Al-CO$_3$-LDH and Zn$_2$Al-Ni(CN)$_4$-LDH. The XRD of Zn$_2$Al-LDH collected from the solution without adding Ni (Figure 5) showed different diffraction peaks from those of Zn$_2$Al-Ni(CN)$_4$-LDH, pointing out to be a mixed phase of Zn$_2$Al-LDH and Zn(CN)$_2$. This observation indicated that Ni(CN)$_4^{2-}$ could be introduced into LDH interlayer, but Zn(CN)$_4^{2-}$ cannot (probably due to its instability), which might be the main reason why adding Ni^{2+} facilitated the removal

12

of CN^-.

As listed in Table 1, Zn/Al molar ratio was 1.92-2.18 in the collected samples, close to the Zn/Al ratio of 2.0, as expected. This indicated that most Zn^{2+} converted from $Zn(CN)_4^{2-}$ was removed in LDH sample. Detail analysis demonstrated that the Ni/Al molar ratio in the solid was 0.10 (Table 1), which was corresponding to approximately 20% LDH intercalated by Ni-CN complex. This was consistent with the co-existing of major CO_3^{2-} and minor $Ni(CN)_4^{2-}$(20%) in the Zn_2Al-LDH interlayer (Figure 2).

3.4. Effects of Experimental Factors on CN Removal.

The precipitation conditions (aging time, pH, CN/Al molar ratio and binary metal in LDH) play an important role in CN removal. As shown in Figure 6A, 92%-95% of CN was removed in 5-10 min. With the increasing aging time to 2 and 18 h, the CN removal percentage was decreased to 88% and 76%. As discussed above, the decrease of CN removal efficiency with the aging time could be largely attributed to the desorption/de-intercalation of free CN^-, since CN^- has a low affinity for LDH [23-25]. This suggests that quick precipitation may simultaneously intercalate/adsorb $Ni(CN)_4^{2-}/CN^-$ into/onto the LDH interlayer/surface, and efficiently remove CN, which was supported by the CN vibration at 2121 cm^{-1} in the FTIR spectrum of the solid sample after 10 min and 18 h treatment (Figure 3).

As shown in Figure 6B, the removal efficiency of CN was 95% at pH 8.0, but then reduced to 60-70% at pH = 9.0-11.0. The decrease at higher pH values could be mainly caused by the competitive adsorption/intercalation of OH^-, which inhibited the

13

removal of CNf. The affinity of OH⁻ and CN⁻ for LDH seemed similar to each other. Since [OH⁻] was 0.1-1.0 mM at pH = 10-11 and the residual CN⁻ was ~ 0.1 mM (2.6 mg/L), the competition adsorption of OH⁻ would be significant. At a lower pH (e.g. < 7.5), there would be some HCN formed that could be readily evaporated, thus pH at 8.0 is practically the optimal pH value for the efficient CN removal. In addition, although the HCN forms at pH = 9.4, the volatilization of HCN was neglected as most CN was transferred in $Ni(CN)_4^{2-}$ which has the high value of $log\beta4$ to inhibit the formation of HCN in LDH precipitation at pH <9.0.

Apart from the aging time and pH, the initial CN/Al molar ratio also affects CN removal. As shown in Figure 6C, CN removal percentage was over 90% at the CN/Al molar ratio $\leq$ 0.5, while the percentage decreased to about 70%, when CN/Al increased to 1.0-2.0. This suggested that efficient CN removal occurred at the CN/Al molar ratio of 0.5 or less.

As shown in Figure 6D, with M(II)/Al (M(II) = Mg, Ni and Zn) and CN/Al molar ratio fixed at 2.0 and 0.5, CN removal percentage was 95% in the case of ZnAl-LDH, but decreased to 79% and 54% in the case of NiAl-LDH and MgAl-LDH. It is our belief that LDH crystal size determines CN removal efficiency. As shown in Figure 7, the crystal size of Zn_2Al-LDH in TEM image was the largest, and that of Mg_2Al-LDH was the smallest. As the surface-adsorbed $CN^-/Ni(CN)_4^{2-}$ can be readily exchanged with solution CO_3^{2-} or NO_3^- within a few minutes [26], more adsorbed CN⁻ on Mg_2Al-LDH and Ni_2Al-LDH were probably exchanged and desorbed into solution, reducing the removal percentage. Therefore, the optimal conditions for the current

14

Ni-assisted CN removal process was quick precipitation of Zn_2Al-LDH in Ni-added Zn-CN solutions at a pH around 8.0 with initial CN/Al ≤ 0.5 after aging for 10 min or short.

Under the optimal conditions, the cost of wastewater treatment was calculated, which mainly involved the addition of aluminum (and extra zinc if necessary) and the precipitation/separation process. The average price of chemicals was 30 RMB (Chinese currency unit) per 500 g and the precipitation/separation process cost 55 RMB per one meter cube. In consequence, it is supposed that the treatment cost of wastewater was 98 RMB per one meter cube.

4. Conclusion

In summary, we presented a co-precipitation strategy to efficiently remove CN and metals via quickly precipitation of LDH with Ni assistance. Over 95% CN was removed from Zn-CN solution and most metals were precipitated as well. This research demonstrated that adding Ni assists the conversion of $CN^-/Zn(CN)_4^{2-}$ to $Ni(CN)_4^{2-}$ and the intercalation of $Ni(CN)_4^{2-}/CN^-$ into larger LDH crystals. The optimal conditions for CN removal are at the pH around 8.0 with initial CN/Al ≤ 0.5 after aging for 10 min. Our results thus suggest that the current strategy is a quick, efficient and promising way to simultaneously treat both Ni and metals/CN rich electroplating wastewaters.

15

References

(1) Wang, Q.; O'Hare, D., Recent Advances in the Synthesis and Application of Layered Double Hydroxide (LDH) Nanosheets. Chem. Rev. 112 (2012) 4124-4155.

(2) Gunjakar, J. L.; Kim, T. W.; Kim, H. N.; Kim, I. Y.; Hwang, S.-J., Mesoporous Layer-by-Layer Ordered Nanohybrids of Layered Double Hydroxide and Layered Metal Oxide: Highly Active Visible Light Photocatalysts with Improved Chemical Stability. J. Am. Chem. Soc.133 (2011) 14998-15007.

(3) Cho, S.; Jung, S.; Jeong, S.; Bang, J.; Park, J.; Park, Y.; Kim, S., Strategy for Synthesizing Quantum Dot-Layered Double Hydroxide Nanocomposites and Their Enhanced Photoluminescence and Photostability. Langmuir 29(2012) 441-447.

(4) Kok-Hui Goha,; Teik-Thye Lima,; Zhili Dong., Application of layered double hydroxides for removal of oxyanions: A review. Water. Res.42(2008) 1343-1368.

(5) Braterman, P. S.; Xu, Z. P.; Yarberry, F., Layered Double Hydroxides(LDHs). In

16

Handbook of Layered Materials, Auerbach, S. M.; Carrado, K. A.; Dutta, P. K., Eds. Marcel Dekker: New York, 2004; p 373.

(6) Taviot-Gueho, C.; Feng, Y. J.; Faour, A.; Leroux, F., Intercalation chemistry in a LDH system: anion exchange process and staging phenomenon investigated by means of time-resolved, in situ X-ray diffraction. Dalton T. 39 (2010) 5994-6005.

(7) Wu, Y. Y.; Bai, H. M.; Zhou, J. Z.; Chen, C. X.; Xu, X.; Xu, Y. F.; Qian, G. R., Thermal and chemical stability of Cu-Zn-Cr-LDHs prepared by accelerated carbonation. Appl. Clay Sci. 42 (2009) 591-596.

(8) Zhou, J. Z.; Wu, Y. Y.; Liu, C.; Orpe, A.; Liu, Q.; Xu, Z. P.; Qian, G. R.; Qiao, S. Z., Effective Self-Purification of Polynary Metal Electroplating Wastewaters through Formation of Layered Double Hydroxides. Environ. Sci. Tech. 44 (2010) 8884-8890.

(9) Xu, Y. F.; Zhang, J.; Zhou, J. Z.; Chen, C.; Liu, Q.; Qian, G. R.; Xu, Z. P., CN and heavy metal removal through formation of layered double hydroxides from mixed CN-containing electroplating wastewaters and pickle acid liquor. Chem. Eng. J. 215 (2013) 411-417.

(10) Dzombak, D. A., Gosh, R. S., and Wong-Chong, G. M., Cyanide in water and soil: Chemistry, risk and management, CRC Press, Boca Raton, FL. 2006, .

(11) Alonso-González, O.; Nava-Alonso, F.; Jimenez-Velasco, C.; Uribe-Salas, A., Copper cyanide removal by precipitation with quaternary ammonium salts. Miner. Eng. 42 (2013) 43-49.

(12) Dash, R. R.; Balomajumder, C.; Kumar, A., Removal of cyanide from water and wastewater using granular activated carbon. Chem. Eng. J. 2009, 146, (3), 408-413.

17

(13) Osathaphan, K.; Boonpitak, T.; Laopirojana, T.; Sharma, V. K., Removal of Cyanide and Zinc–Cyanide Complex by an Ion-Exchange Process. Water Air Soil Pollut. 194 (2008) 179-183.

(14) Zhang, J.; Xu, Y. F.; Liu, J. Y.; Zhou, J. Z.; Xu, Z. P.; Qian, G. R., $Fe(CN)_6^{3-}/Fe(CN)_6^{4-}$ redox in the interlayer determined by the charge density of ZnnCr-layered double hydroxides. J. Solid State Chem. 198 (2013) 506-510.

(15) Speight, J. G., Lange's Handbook of Chemistry, Sixteenth Edition. McGraw-Hill Education LLC: New York, 2005.

(16) Fang, W. Layered Double Hydroxides: Synthesis, Characterization, and Interaction of Mg-Al Systems with Intercalated Tetracyanonickelate(II). University of North Texas, Denton,Texas, 2004.

(17) Acheampong, M. A.; Meulepas, R. J. W.; Lens, P. N. L., Removal of heavy metals and cyanide from gold mine wastewater. J.Chem. Technol. Biot. 85 (2010) 590-613.

(18) Xie, F.; Dreisinger, D.; Doyle, F., A Review on Recovery of Copper and Cyanide From Waste Cyanide Solutions. Min. Proc. Ext. Met. Rev. 34(2013)387-411.

(19) Water quality-Determination of cyanide-Volumetric and spectrophotometry method HJ 484-2009, In: Ministry of Environmental Protection of PRC: Beijing, 2009.

(20) Sharpe, V. A. G., The Chemistry of Cyano Complexes of the Transition Metals. Academic Press: London-New York-San Francisco, 1976.

(21) Coleman, J. S.; Petersen, H.; Penneman, R. A., Study of the $Ni(CN)_4^{2-}$ and

18

Ni(CN)$_5$$^{3-}$ Equilibrium by Electronic and Vibrational Absorption Spectra; Effect of Fluoride Ion. Inorg. Chem. 4 (1965) 135-139.

(22) Jones, L. H., Vibrational spectra of dipotassium tetrakis(cyano-C)zincate, dipotassium tetrakis(cyano-C)cadmate, and dipotassium tetrakis(cyano-C)mercurate. Inorg. Chem. 13 (1974) 2289-2290.

(23) Lopez-Salinas, E.; Tomita, N.; Matsui, T.; Suzuki, E.; Ono, Y., Reactivity of interstitial [NiCl$_4$]$^{2-}$ complex anions in a Mg Al hydrotalcite-like clay towards alkyl bromides in the liquid phase. J. Mol. Catal. 81(1993) 397-405.

(24) Suzuki, E.; Inoue, A.; Ono, Y.; Reaction of Interstitial Cyanide Ions in a Hydrotalcite-like Material with Organic Chlorides. Chem. Lett. 27 (1998) 1291-1292.

(25) Hoshino, M.; Shimada, H.; Organic reactions with layered double hydroxide-intercalated inorganic nucleophilic reagents. J. Adv. Sci. 7 (1995) 51-51.

(26) Roeffaers, M. B.; Sels, B. F.; Loos, D.; Kohl, C.; Mullen, K.; Jacobs, P. A.; Hofkens, J.; De Vos, D. E., In situ space- and time-resolved sorption kinetics of anionic dyes on individual LDH crystals. Chem.Phys.Chem. 6 (2005) 2295-2299.

19

Table 1 The metal removal rate and the composition information of collected solids

and residual solutions before and after Ni-assisted LDH precipitation .

Treatment	Metal Removal (%)			Molar ratio in collected samples		CN content and composition in the residual solution		Final pH
	Ni	Zn	Al	Zn/Al	Ni/Al	Total CN (mg/L, CNt)	CNf%[a]	
No treatment	N.A.	N.A.	N.A.	N.A.	N.A.	25.0	55.8	12.3
Ni addition	N.A.	N.A.	N.A.	N.A.	N.A.	24.8	18.0	12.0
LDH 10 min[b]	N.A.	89	87	2.18	N.A	7.41	49.1	8.1
LDH-Ni 10 min	73	86	96	1.92	0.10	1.19	15.1	8.1
LDH-Ni 18 h	72	96	95	2.17	0.10	5.95	53.3	7.8

[a] CNf% represents the percent of free CN in total CN, e.g. [CNf]/[CNt]×100%, [CNf] + [CNc] = [CNt], where CNc represents the concentration of complex CN$^-$.
[b] The LDH precipitation without Ni addition was performed for 10 min.

20

Figure captions

Scheme 1 The block diagram of the treatment steps with the sequence and associated

conditions

Figure 1 FTIR spectra of aqueous KCN solution, and CN complexes in Zn-CN

solution and $Ni(NO_3)_2$-added Zn-CN solution.

Figure 2 XRD patterns of collected LDH precipitates under various conditions. The

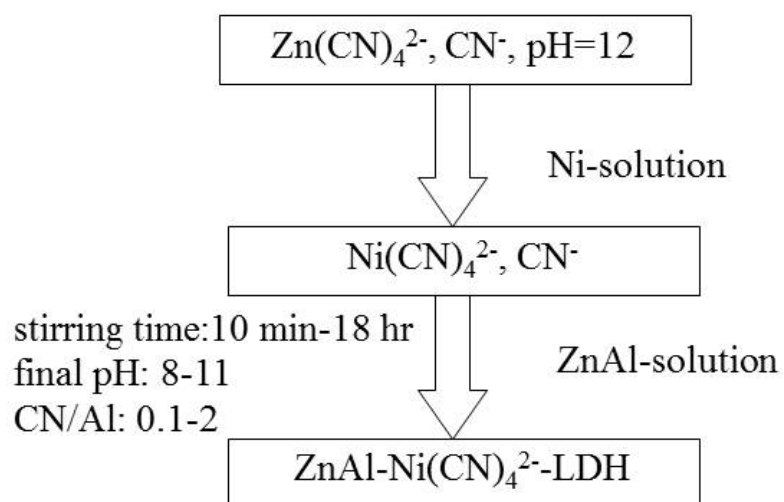band of complex CN marked with star (*) is probably due to impurity Ni in

solution.

Figure 3 FTIR spectra of Zn_2Al-CO_3-LDH (A), $Zn_2Al-Ni(CN)_4$-LDH@18 h (B), and

@10 min (C), and Zn_2Al-LDH without adding Ni (D).

Figure 4 XRD pattern of the solid sample after Zn_2Al-LDH precipitation without Ni

assistance.

Figure 5 (A) SEM image of Zn_2Al-LDH collected after the CN removal with Ni

addition; (B) Schematic intercalation of $Ni(CN)_4^{2-}$ into LDH.

Figure 6 CN removal efficiency as a function of stirring time (A), pH (B), initial

CN/Al molar ratio (C) and bivalent cation in LDH (D)

Figure 7 TEM images of Mg_2Al-LDH(A), Ni_2Al-LDH(B), Zn_2Al-LDH(C) collected

after the CN removal.

21

Scheme 1 The block diagram of the treatment steps with the sequence and associated
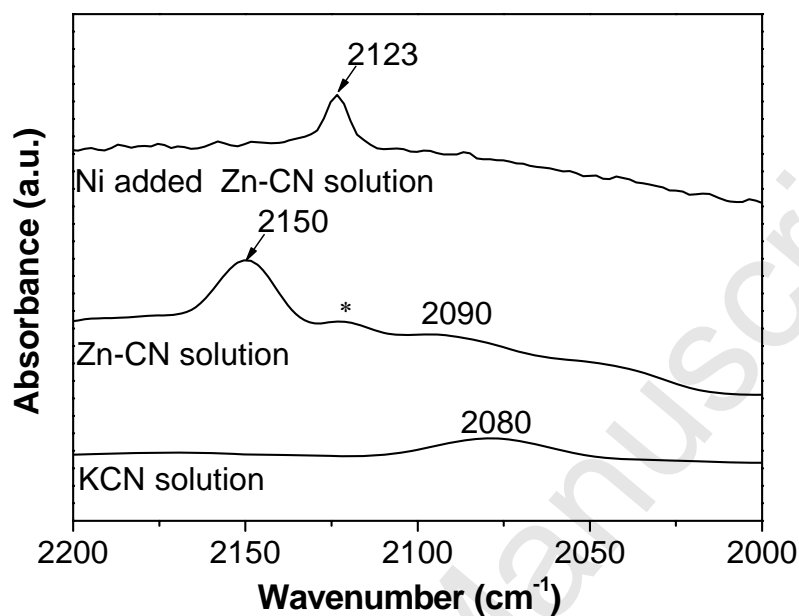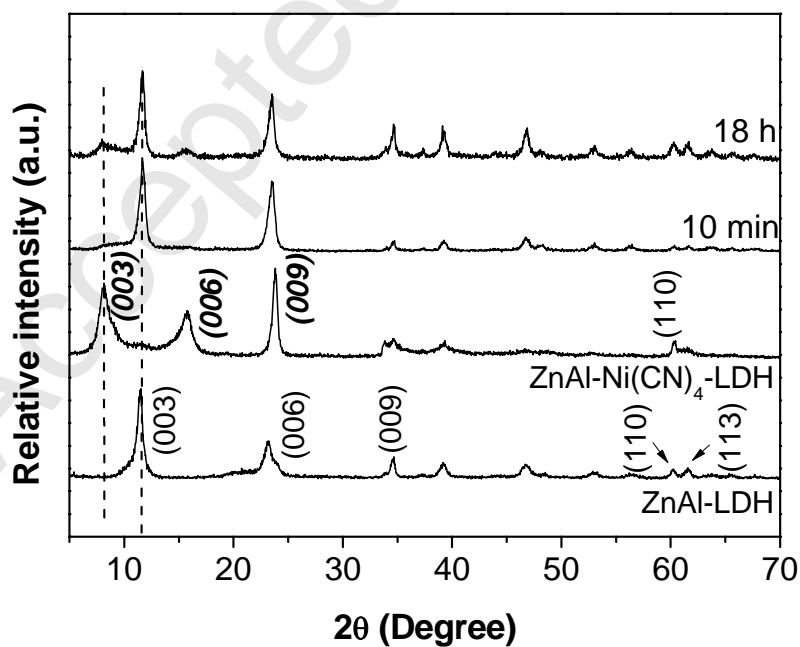
conditions

Figure 1 FTIR spectra of aqueous KCN solution, and CN complexes in Zn-CN solution and $Ni(NO_3)_2$-added Zn-CN solution

Figure 2 XRD patterns of collected LDH precipitates under various conditions. The band of complex CN marked with star (*) is probably due to impurity Ni in simulated solution.
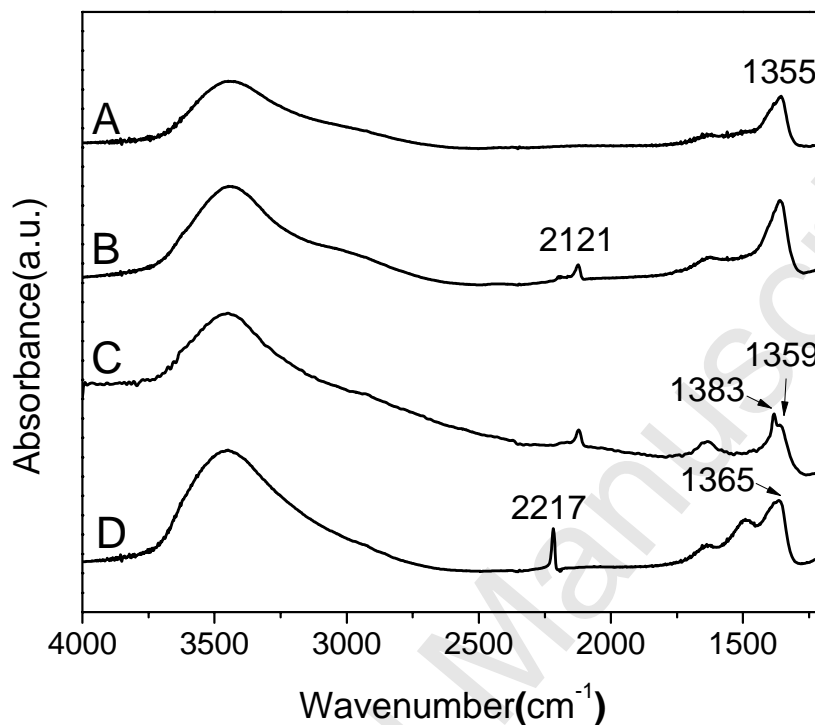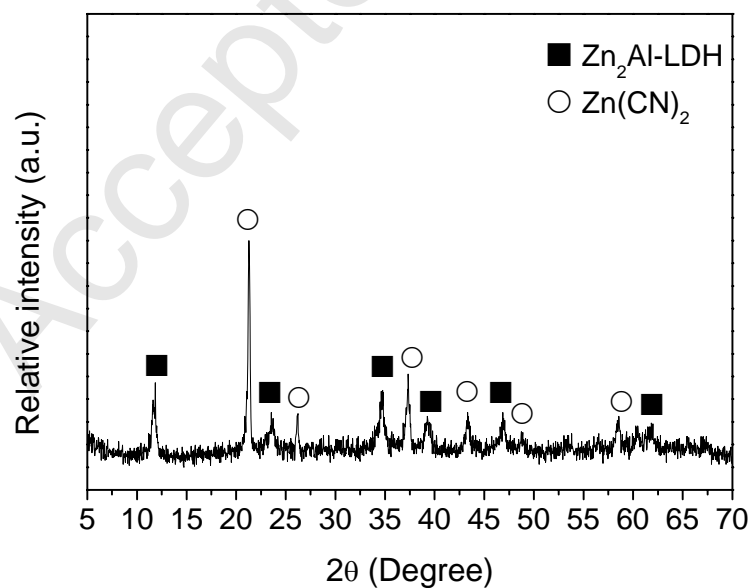
23

Figure 3 FTIR spectra of Zn_2Al-CO_3-LDH (A), $Zn_2Al-Ni(CN)_4-LDH@18$ h (B), and @10 min (C), and $Zn_2Al-LDH$ without adding Ni (D).

Figure 4 XRD pattern of the solid sample after $Zn_2Al-LDH$ precipitation without Ni assistance.

24

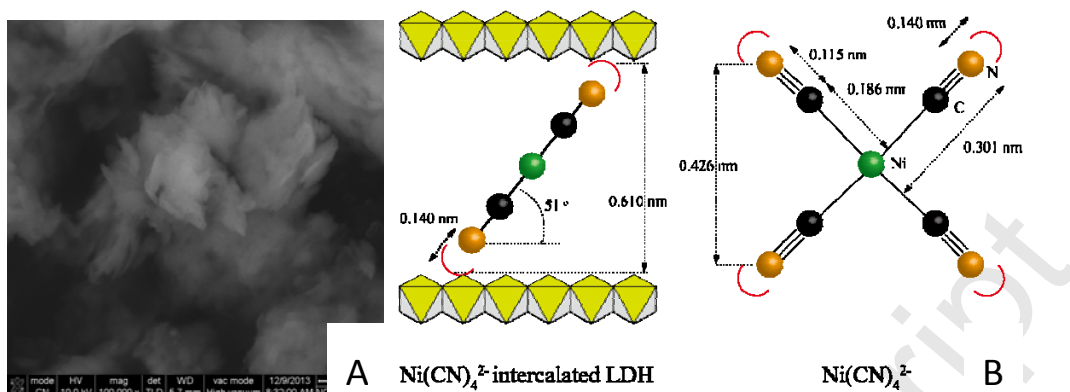Figure 5 (A) SEM image of Zn_2Al-LDH collected after the CN removal with Ni addition; (B) Schematic intercalation of $Ni(CN)_4^{2-}$ into LDH.
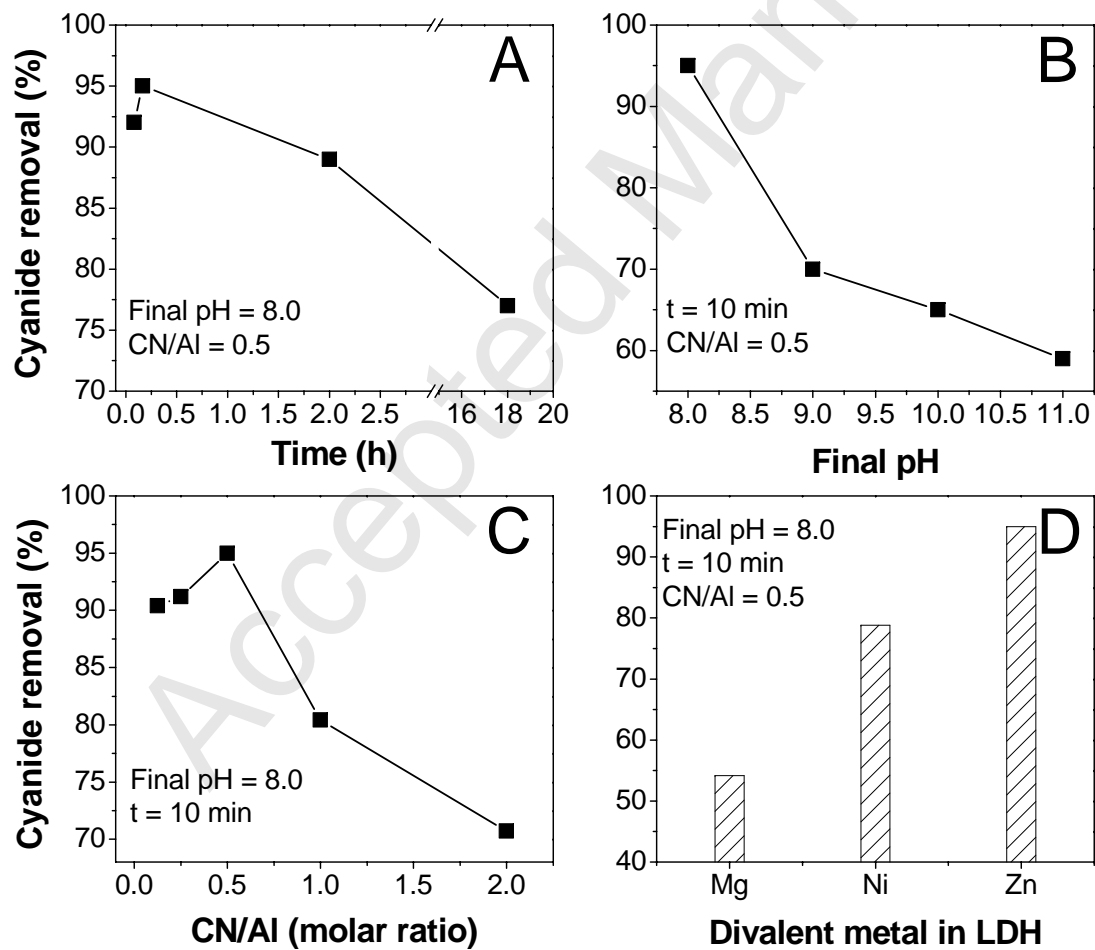
25

Figure 6 CN removal efficiency as a function of stirring time (A), pH (B), initial CN/Al molar ratio (C) and bivalent cation in LDH (D)
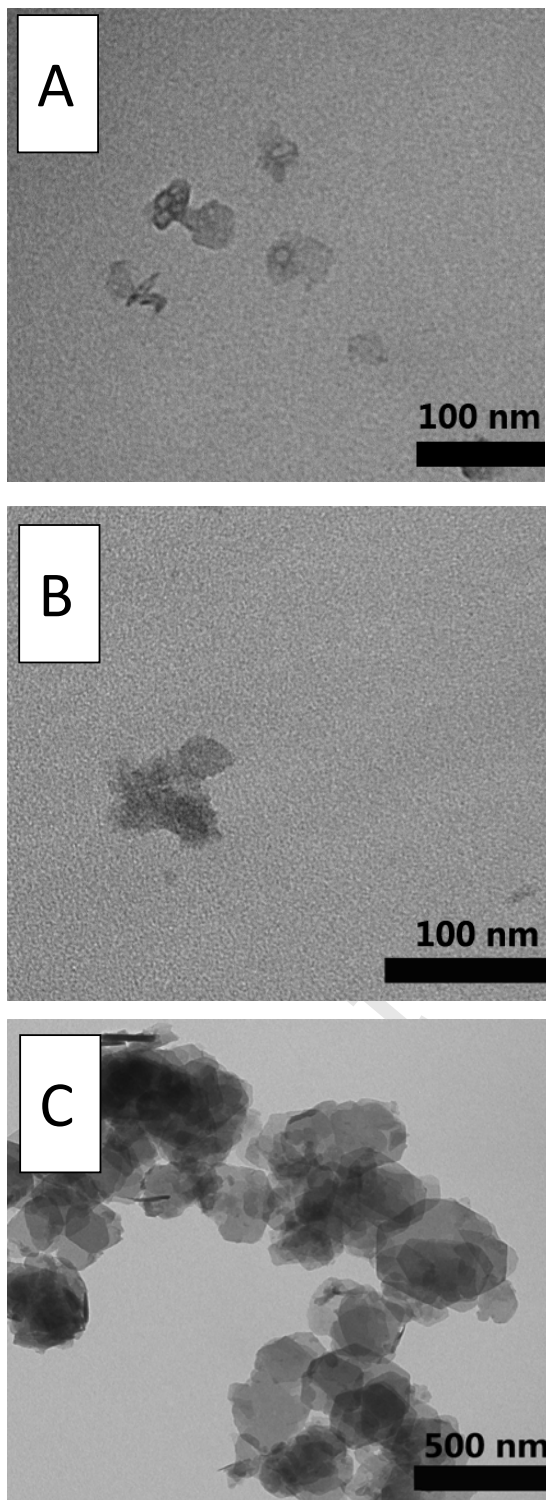
Figure 7 TEM images of Mg$_2$Al-LDH(A), Ni$_2$Al-LDH(B), Zn$_2$Al-LDH(C) collected after the CN removal.

28

Graphical abstract

29